Decomposition and Isomerization of 1,2-Benzisoxazole: Single-Pulse Shock-Tube Experiments, Quantum Chemical and Transition-State Theory Calculations

Assa Lifshitz,* Carmen Tamburu, Aya Suslensky, and Faina Dubnikova

Department of Physical Chemistry, The Hebrew University of Jerusalem, Jerusalem 91904, Israel

Received: May 22, 2006; In Final Form: August 20, 2006

Isomerization and decomposition of 1,2-benzisoxazole were studied behind reflected shock waves in a pressurized driver, single-pulse shock tube. It isomerizes to *o*-hydroxybenzonitrile, and no fragmentation is observed up to a temperature where the isomerization is almost complete (∼1040 K at 2 ms reaction time). The isomerization experiments in this investigation covered the temperature range 900−1040 K. The lack of fragmentation is in complete contrast to the thermal behavior of isoxazole, where no isomerization was observed and the main decomposition products over the same temperature range were carbon monoxide and acetonitrile. In a series of experiments covering the temperature range 1190−1350 K, a plethora of fragmentation products appear in the post shock samples of 1,2-benzisoxazole. The product distribution is exactly the same regardless of whether the starting material is 1,2-benzisoxazole or *o*-hydroxybenzonitrile, indicating that over this temperature range the 1,2-benzisoxazole has completely isomerized to *o*-hydroxybenzonitrile prior to fragmentation. Two potential energy surfaces that lead to the isomerization were evaluated by quantum chemical calculations. One surface with one intermediate and two transition states has a high barrier and does not contribute to the process. The second surface is more complex. It has three intermediates and four transition states, but it has a lower overall barrier and yields the isomerization product *o*-hydroxybenzonitrile at a much higher rate. The unimolecular isomerization rate constants k_∞ at a number of temperatures in the range of 900−1040 K were calculated from the potential energy surface using transition-state theory and then expressed in an Arrhenius form. The value obtained is $k_{first} = 4.15 \times 10^{14} \exp(-51.7 \times 10^3/RT)\ s^{-1}$, where R is expressed in units of cal/(K mol). The calculated value is somewhat higher than the one obtained from the experimental results. When it is expressed in terms of energy difference it corresponds of ca. 2 kcal/mol.

I. Introduction

1,2-Benzisoxazole is one of three isomers where a five-membered ring, containing oxygen and nitrogen, is fused to a benzene ring. The three isomers differ from one another by the location of the nitrogen and oxygen atoms with respect to the benzene ring and with respect to one another.

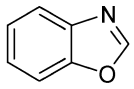

benzoxazole

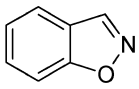

1,2-benzisoxazole

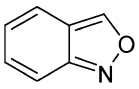

2,1-benzisoxazole (anthranil)

We recently published detailed investigations on the decompositions and isomerizations of 2,1-benzisoxazole[1] and benzoxazole.[2] These two compounds differ a great deal in their stability and reactivity. The stability of the three isomers and their reactivity depend on the extent of the resonance of the benzene ring[3,4] and on the relative position of the nitrogen with respect to the oxygen. As can be seen in the above diagram, benzoxazole has no weak N−O bond and the resonance of the benzene ring is unaffected by the fused five-membered ring. 2,1-Benzisoxazole, on the other hand, is much less stable. It has both a weak N−O bond and loss of the benzene resonance stabilization. The difference in their heat of formation is higher than 30 kcal/mol at 298 K.[3] The thermal stability of 1,2-benzisoxazole, which is the subject of this investigation, is somewhere between the other two isomers. It has a weak N−O bond, but the benzene stabilization energy is not impaired. As the initiation reaction involves cleavage of the N−O bond, isomerization of 1,2-benzisoxazole to *o*-hydroxybenzonitrile is thus expected to take place at a much lower temperature than that of benzoxazole, which isomerizes to the same isomerization product.

In this article we present experimental results over two temperature ranges 900−1040 and 1190−1350 K. We also present quantum chemical calculations of reaction pathways of the isomerization of 1,2-benzisoxazole to *o*-hydroxybenzonitrile. Rate constants are estimated on the basis of the calculated potential energy surfaces using transition-state theory and compared to the experimental results obtained by the single-pulse shock-tube technique.

II. Experimental Section

1. Shock Tube. The thermal decomposition and isomerization of benzisoxazole were studied behind reflected shock waves in a pressurized driver, 2 in. i.d. single-pulse shock tube. The driven section was 4 m long, and the driver had a variable length up to a maximum of 2.7 m and could be varied in small steps in order to tune for the best cooling conditions. A 36-L dump tank was connected to the driven section near the diaphragm holder in order to quench transmitted shocks. The tube, gas handling system, reaction mixture bulbs, and transfer tubes were all maintained at 100 °C with an accuracy of ±2 °C. Total densities

* To whom correspondence should be addressed. E-mail: Assa@vms.huji.ac.il.

10.1021/jp063125k CCC: $33.50 © 2006 American Chemical Society
Published on Web 09/27/2006

behind the reflected shock, C_5, in all the experiments were around 3×10^{-5} mol/cm^3. Cooling rates were approximately 5×10^5 K/s.

2. Reflected Shock Temperatures. Reflected shock temperatures were determined from the extent of decomposition of two internal standards: cyclopropane carbonitrile (c-C_3H_5-CN) and 1,1,1-trifluoroethane (CH_3CF_3), which were added in small quantities to the reaction mixtures to serve as chemical thermometers. Cyclopropane carbonitrile was used over the temperature range 900−1040 K. It isomerizes to *cis*- and *trans*-crotonitrile ($CH_3CH{=}CHCN$) and vinylacetonitrile ($CH_2{=}CH{-}CH_2CN$) with an overall rate constant of $10^{14.58}$ exp($-57.8 \times 10^3/RT$) s^{-1} corresponding to the above-mentioned temperature and pressure of this investigation.[5] 1,1,1-Trifluoroethane decomposes to $CH_2{=}CF_2 + HF$ in a first-order unimolecular reaction that has a rate constant of: $k_{first} = 10^{14.85}$ exp($-74.05 \times 10^3/RT$) s^{-1}, where R is expressed in units of cal/(K mol).[6] It was used over the temperature range of ∼1190−1350 K.

Reflected shock temperatures were then calculated from the relation

$$T = -(E/R)/\left[\ln\left\{-\frac{1}{A \times t}\ln(1-\chi)\right\}\right]$$

where t is the reaction dwell time, approximately 2 ms, A and E are the Arrhenius parameters of the standard reaction, and χ is the extent of reaction (isomerization or decomposition) defined as

$$\chi = [\sum(\text{products})]_t/\{[\sum(\text{products})]_t + [\text{reactant}]_t\}$$

Density ratios were calculated from the measured incident shock velocities using the three conservation equations and the ideal gas equation of state.

3. Materials and Analysis. After pumping down a 12 L heated glass bulb to ∼10^{-5} Torr, an amount of liquid corresponding to 0.5% 1,2-benzisoxazole was injected into the evacuated bulb that was then filled to one atmosphere with argon containing 0.08% of the internal standard, CH_3CF_3 or c-C_3H_5-CN, depending upon the temperature range of the experiments. The bulb served as storage for the reaction mixture.

Gas chromatographic analyses with flame ionization and nitrogen phosphor detectors (FID, NPD) were used to determine the composition of post shock mixtures. Temperature-programmed Porapak N and Tenax columns at various lengths were used for product separation.

The concentration of the carbon monoxide (in the high-temperature series) was evaluated from nitrogen−oxygen mass balance considerations assuming a minimal loss of material if at all. No other oxygen-containing species were analyzed in the post shock samples. Typical chromatograms showing traces obtained on the two detectors are given in Figures 1−3.

III. Experimental Results

1. High-Temperature Experiments. In our first series of experiments we ran 13 tests covering the temperature range 1190−1350 K trying to measure the isomerization rate 1,2-benzisoxazole → *o*-hydroxybenzonitrile. Over this temperature range we found *o*-hydroxybenzonitrile as well as a plethora of fragmentation products, as can be seen in Figure 4, but no 1,2-benzisoxazole could be detected in the post shock samples. It was not clear at that stage whether fragmentation was due to the reaction that took place parallel to the isomerization or whether the isomerization to *o*-hydroxybenzonitrile occurred in a very short time so that we measured nothing but the

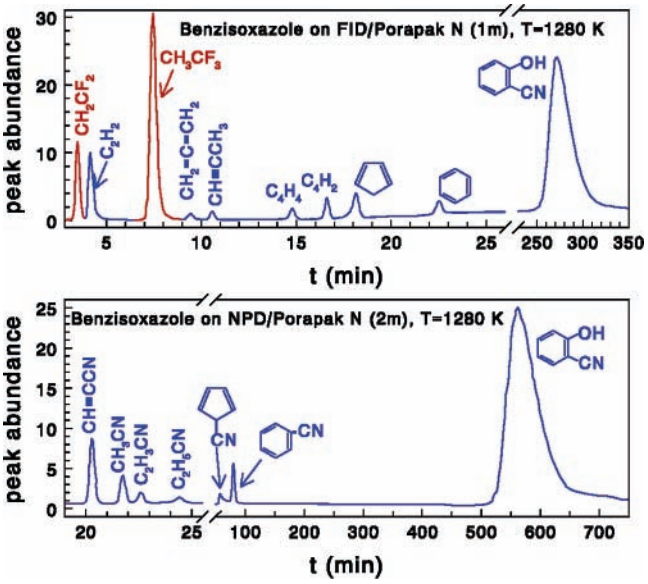

Figure 1. Gas chromatograms showing the fragmentation products of 1,2-benzisoxazole. (Top) FID/Porapak N. (Bottom) NPD/Porapak N. The peaks shown in red are those of CH_3CF_3 and $CH_2{=}CF_2$ from the ratio of which the temperature behind the reflected shock is calculated.

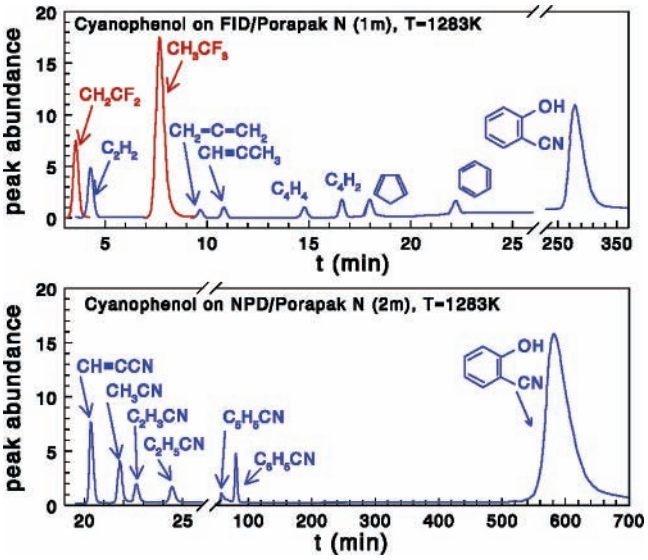

Figure 2. Gas chromatograms showing the fragmentation products of *o*-hydroxybenzonitrile. (Top) FID/Porapak N. (Bottom) NPD/Porapak N.

fragmentation pattern of the latter. To clarify this point, we ran 10 tests where the starting material was *o*-hydroxybenzonitrile. Comparison between formation rates of products from the decomposition of these two compounds is shown, as an example, for C_2H_2, C_6H_6, C_2H_3CN, and C_5H_5CN in Figure 5. As can be seen, within the limit of experimental error, the production rates of these four products is practically the same regardless of whether the starting material was 1,2-benzisoxazole or *o*-hydroxybenzonitrile. This clearly indicates that 1,2-benzisoxazole isomerizes to *o*-hydroxybenzonitrile without fragmentation at much lower temperatures than those covered in these series of experiments. It should be mentioned that both benzoxazole and 1,2-benzisoxazole undergo fragmentation by electron impact also not prior to isomerization to *o*-hydroxybenzonitrile. The main products are CO and HCN.[7]

2. Low-Temperature Experiments. To measure the isomerization rate of benzisoxazole → *o*-hydroxybenzonitrile 30 tests were run covering the temperature range 900−1040 K. As the

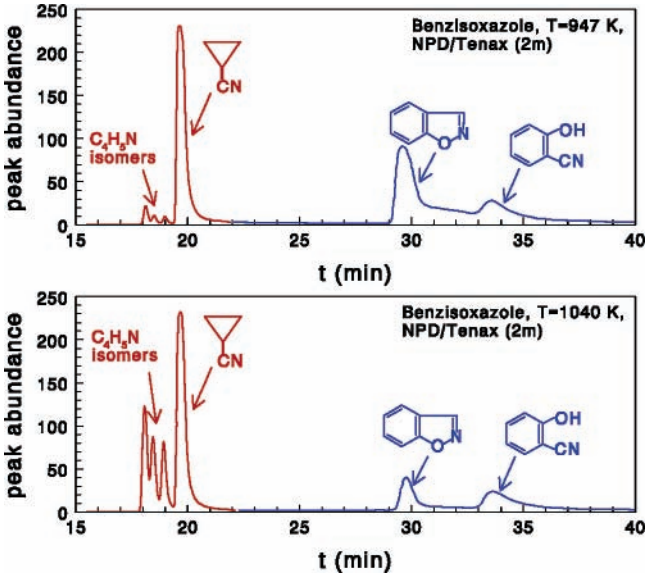

Figure 3. Gas chromatograms showing the fragmentation products of 1,2-benzisoxazole taken at two different temperatures using cyclopropane carbonitrile (in red) as a chemical thermometer. No fragmentation is observed in these temperatures.

equilibrium of isomerization is very high, the back reaction can be neglected and considered as an irreversible unimolecular reaction. Figure 6 is an Arrhenius plot of the isomerization rate constant. The solid lines are the result of the quantum chemical calculations as will be discussed later.

IV. Quantum Chemical and Rate Constant Calculations

1. Quantum Chemical Calculations. We used the Becke three-parameter hybrid method[8] with Lee−Yang−Parr correlation functional approximation (B3LYP)[9] and the Dunning correlation consistent polarized valence double ζ (cc-pVDZ) basis set.[10] Structure optimization of the reactants and products was done using the Berny geometry optimization algorithm.[11] For determining transition-state structures, we used the combined synchronous transit-guided quasi-Newton (STQN) method.[12] The higher level (CI) calculations were done using these geometries.

All calculations were performed without symmetry restrictions**.** Vibrational analyses were done at the same level of theory to characterize the optimized structures as local minima or transition states. Calculated vibrational frequencies and entropies (at B3LYP level) were used to evaluate preexponential factors of the reactions under consideration. All calculated frequencies, zero-point energies, and thermal energies are of harmonic oscillators. The calculations of the intrinsic reaction coordinate (IRC), to check whether the transition states under consideration connect the expected reactants and products, were done at the B3LYP level of theory with the same basis set as that used for the stationary point optimization. These calculations were done on all transition states.

The points on the potential energy surfaces, having a biradical character, were located by the unrestricted uB3LYP method using guess wave function, destroying the $\alpha-\beta$ and spatial symmetry. We used an open-shell singlet approximation for the biradical structures.

To determine the multireference character of the biradical transition states and intermediates, we calculated their T_1 value, which according to diagnostics introduced by Lee and Taylor reflects the extent of the multireference character of the species on the surface.[13] In five species the T_1 values were considerably

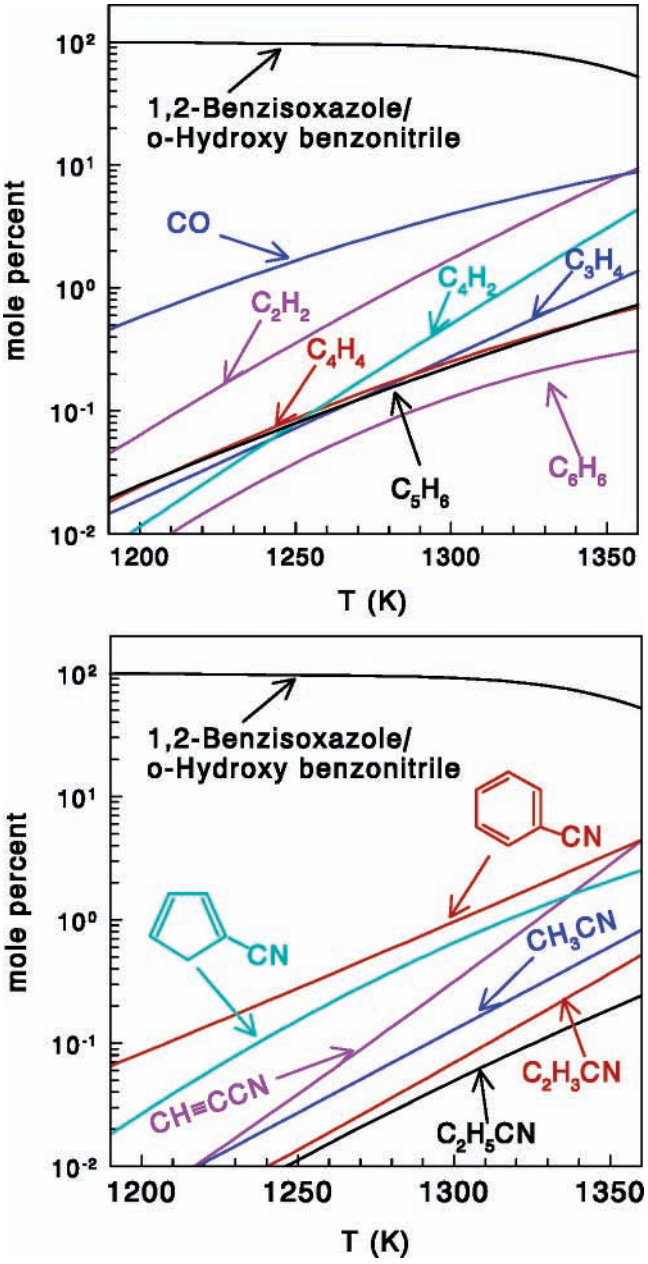

Figure 4. General product distribution in the decomposition of 1,2-benzisoxazole/*o*-hydroxybenzonitrile over the temperature range 1200−1350 K. The distribution is the same regardless of whether the starting material is 1,2-benzoxasole or *o*-hydroxybenzonitrile.

higher than 0.02, a value that is being considered as the highest value below which the multireference character is negligible.[14] The calculated values were between 0.04 and 0.05. However, it has been shown[15−17] that the coupled cluster theory for CI calculations, with inclusion of perturbative estimates for the effects of triple excitations, can compensate for inadequacies in the single-determinant reference. In view of these findings, we used the coupled cluster theory CCSD(T) for configuration interaction calculations at B3LYP geometry. The CCSD(T) calculations were performed with the frozen core approximation. All of the reported relative energies include zero-point energy correction (ZPE).

The DFT and QCISD(T) computations were carried out using the Gaussian-98 program package[18] and done on a DEC Alpha XP1000 1/667 professional workstation.

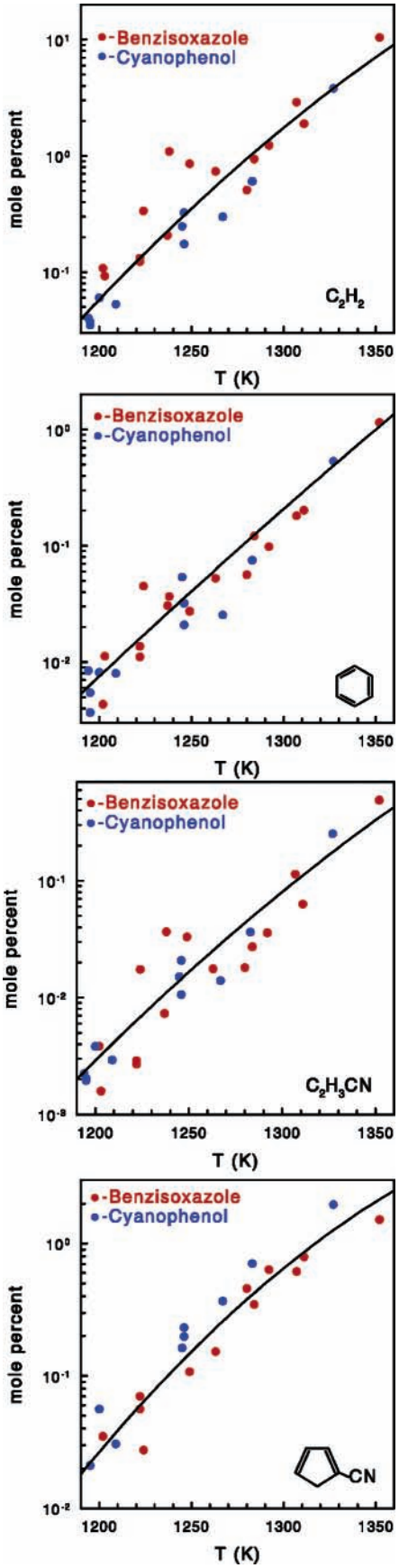

Figure 5. Detailed distribution of four reaction products in the decomposition of 1,2-benzisoxazole/*o*-hydroxybenzonitrile over the temperature range 1200−1350 K. The red points represent the decomposition of 1,2-benzisoxazole, and the blue ones represent the decomposition of *o*-hydroxybenzonitrile. Within the limit of experimental error there is no difference between the two series of points.

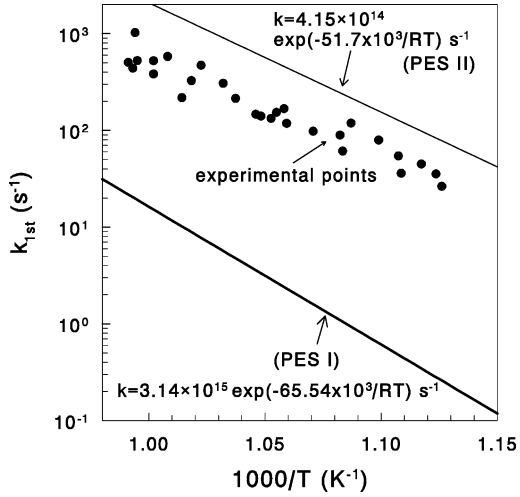

Figure 6. Comparison between the experimental and calculated points of the Arrhenius rate constant of the isomerization: 1,2-benzisoxazole → *o*-hydroxybenzonitrile. The experimental points (filled circles) are in reasonable agreement with rate constant calculated on the basis of surface II.

2. Rate Constant Calculations. To evaluate the high-pressure limit first-order rate constants from the quantum chemical calculations the relation

$$k_\infty = \sigma(kT/h)\exp(\Delta S^{\ddagger}/R)\exp(-\Delta H^{\ddagger}/RT) \qquad (1)$$

was used,[19,20] where h is Planck's constant, k is the Boltzmann factor, σ is the degeneracy of the reaction coordinate, and $\Delta H^{\ddagger}$ and $\Delta S^{\ddagger}$ are the temperature-dependent enthalpy and entropy of activation respectively. Since we deal with unimolecular reactions, $\Delta H^{\ddagger} = \Delta E^{\ddagger}$, where $\Delta E^{\ddagger}$ is the energy difference between the transition state and the reactant. $\Delta E^{\ddagger}$ is equal to $\Delta E_{\text{total}}^{\circ} + \Delta E_{\text{thermal}}$, where $\Delta E_{\text{total}}^{\circ}$ is obtained by taking the difference between the total energies of the transition state and the reactant and $\Delta E_{\text{thermal}}$ is the difference between the thermal energies of these species.

V. Results of the Quantum Chemical Calculations

1. Potential Energy Surface I. A potential energy surface of 1,2-benzisoxazole → *o*-hydroxybenzonitrile isomerization is shown in Figure 7. The energetics and other parameters relevant to this surface are shown in Table 1. Selected structural parameters of the species on the surface are shown in Table 2. The surface contains two transition states and one intermediate.

The first stage is a concerted process where rupture of the N(2)−O(1) bond and 1,2-H-atom migration from C(3) to N(2) occur simultaneously, producing intermediate INT1 (Figure 7). The result of the N−O bond breaking is shortening of the O(1)−C(8) bond from a single bond (1.354 Å) to a double bond (1.241 Å) already in the transition-state TS1. The energy barrier of this step is 62 kcal/mol at the CCSD(T)//B3LYP/cc-pVDZ level of the theory. This barrier can be compared with the barrier of the similar transition state (including N−O bond breaking and H-atom migration) in isoxazole calculated at the QCISD(T)//B3LYP/6-311++G** level which is 58.5 kcal/mol.[21]

The energy level of INT1 (6-iminomethylene-1,3-cyclohexadiene-5-one) relative to 1,2-benzisoxazole is only 9.45 kcal/mol. This is somewhat unexpected result since the resonance of the benzene ring in INT1 is completely lost. A similar phenomenon, however, was observed in the isomerization of dihydrobenzofuran,[22] where loss of the resonance of the benzene ring is compensated to a large extent by formation of a strong

TABLE 1: Total Energies E_{total} (in au), Zero-Point Energies, Relative Energies ΔE,[a] Imaginary Frequencies,[b] and Entropies[c] of the Species on the 1,2-Benzisoxasole → *o*-Hydroxybenzonitrile Potential-Energy Surface

	uB3LYP						uCCSD(T)	
species	E_{total}	ΔE^a	ZPE	S[c]	$\langle S^2 \rangle$	ν^b	E_{total}	ΔE^a
1,2-benzisoxazole	−399.709351	0.0	65.93	77.67			−398.615024	0.0
potential energy surface I (Figure 7)								
TS1	−399.607628	58.11	60.21	83.98		(i-1038)	−398.507185	61.95
INT1	−399.694005	7.42	63.72	84.81			−398.596435	9.45
TS2	−399.668715	21.07	62.00	81.57		(i-624)	−398.567645	25.80
potential energy surface II (Figure 8)								
TS3	−399.642122	38.61	62.35	80.56	0.8032	(i-428)	−398.541096	42.81
INT2	−399.645714	36.41	62.41	84.90	1.0367		−398.548715	38.09
TS4	−399.638819	40.41	61.88	82.57	1.0361	(i-123)	−398.543699	40.19
INT3	−399.648823	35.30	63.25	83.49	0.0		−398.562675	30.17
TS5	−399.634010	43.32	61.97	83.47	0.4962	(i-507)	−398.548413	37.84
INT4	−399.650862	33.36	62.59	84.60	1.0357		−398.563606	28.93
TS6	−399.633356	41.93	60.17	81.73	0.5998	(i-1981)	−398.526507	49.79
o-hydroxybenzonitrile	−399.742953	−22.09	64.93	83.57			−398.654752	−25.93

[a] Relative energies in kcal/mol. $\Delta E = \Delta E_{total} + \Delta(ZPE)$. [b] Imaginary frequency in cm^{-1}. [c] Entropies at 298 K in cal/(K·mol).

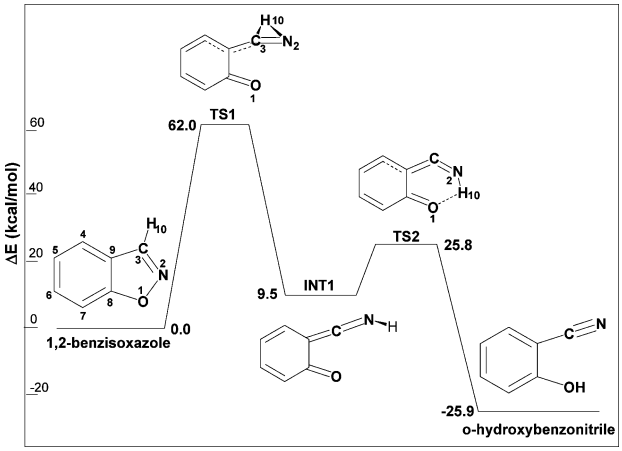

Figure 7. Reaction pathway for 1,2-benzisoxazole → *o*-hydroxybenzonitrile isomerization on potential energy surface I. Relative energies (in kcal/mol) are calculated at the CCSD(T)//B3LYP/cc-pVDZ level of theory. The surface has one intermediate and two transition states, its barrier is high, and it thus does not contribute to the overall isomerization rate.

TABLE 2: Several Structural Parameters of the Species Involved in the Reaction 1,2-Benzisoxazole → *o*-Hydroxybenzonitrile (surface I) Calculated at the B3LYP/cc-pVDZ Level of Theory

parameter[a]	1,2-benz-isoxazole	TS1	INT1	TS2	*o*-hydroxy-benzonitrile
O(1)−N(2)	1.406	2.569			
N(2)−C(3)	1.307	1.228	1.210	1.200	1.166
C(3)−C(9)	1.437	1.381	1.346	1.368	1.432
C(9)−C(4)	1.406	1.416	1.449	1.416	1.409
C(4)−C(5)	1.391	1.373	1.360	1.373	1.390
C(5)−C(6)	1.414	1.427	1.444	1.424	1.403
C(6)−C(7)	1.393	1.373	1.362	1.373	1.392
C(7)−C(8)	1.398	1.451	1.465	1.447	1.401
C(8)−C(9)	1.403	1.498	1.502	1.519	1.416
C(8)−O(1)	1.354	1.241	1.230	1.247	1.352
C(3)−H(10)	1.089	1.240			
N(2)−H(10)		1.436	1.025	1.070	
O(1)−H(10)				1.928	0.973

[a] Distances are in Angstroms. Atom numbering is shown in Figure 7.

C═O bond. In the case of 1,2-benzisoxazole there is even an additional stabilization of the intermediate due to conjugation in the C═C═NH bond that is formed in the intermediate INT1.

The second step of the 1,2-benzisoxazole isomerization is an additional H-atom migration from N(2) to O(1) toward formation of *o*-hydroxybenzonitrile with a barrier of ∼16 kcal/mol.

The relatively high barrier of the rate-determining step, 1,2-benzisoxazole → INT1 via transition-state TS1 (62 kcal/mol), is a combination of two processes, namely, N−O bond cleavage and H-atom migration, and is thus considerably higher than just the N−O bond energy. Since the calculated isomerization rate constant based on this surface is much lower than the experimental results (Figure 6), we decided to search for an additional surface where the first step involves cleavage of the N−O bond but without H-atom migration.

2. Potential Energy Surface II. Such a potential energy surface where the N−O bond is cleaved prior to H-atom migration was indeed found and is shown in Figure 8. The energetics and other parameters relevant to this surface are shown in Table 1. Selected structural parameters of the species on the surface are shown in Table 3. The surface contains four transition states and three intermediates. N−O bond cleavage appears as the first step on the surface and leads to the intermediate INT2 via transition-state TS3. The energy level of TS3 is 42.8 kcal/mol at the uCCSD(T)//uB3LYP//cc-pVDZ level of theory above that of 1,2-benzisoxazole as compared to the value of 62.0 kcal/mol in the previous surface.

Both the transition-state TS3 and the intermediate INT2 on this surface are biradical species. The N−O bond is practically broken, where the O(1)−N(2) distance is 2.374 Å in TS3 and 2.772 Å in INT2 (compared to 1.307 Å in benzisoxazole). The excess electron density is located mainly on both O(1) and N(2). The initial bond orders of the C(8)−O(1) single bond (1.354 Å) and the C(3)−N(2) double bond (1.307 Å) change to bond orders of ∼1.5 (1.248 Å) and ∼2.5 (1.259 Å), respectively. As a result, the aromaticity of the fused benzene ring in INT2 is impaired.

To produce *o*-hydroxybenzonitrile from INT2, the hydrogen atom H(10) has to move from C(3) to O(1). To facilitate the process, the CH═N group in INT2 must rotate around the C(3)−C(9) bond so that H(10) approaches O(1) toward formation of an O−H bond. This process, which is expected to be rather straightforward, turns out to be more complex. The calculations show that this rotation, namely, going from INT2 to INT4, takes place via formation and cleavage of the C(9)−N(2) bond so that INT3 is needed as an additional intermediate. Finally, INT4, with the barrier of ∼21 kcal/mol, produces *o*-hydroxybenzonitrile via transition-state TS6 (Figure 8). The overall barrier from

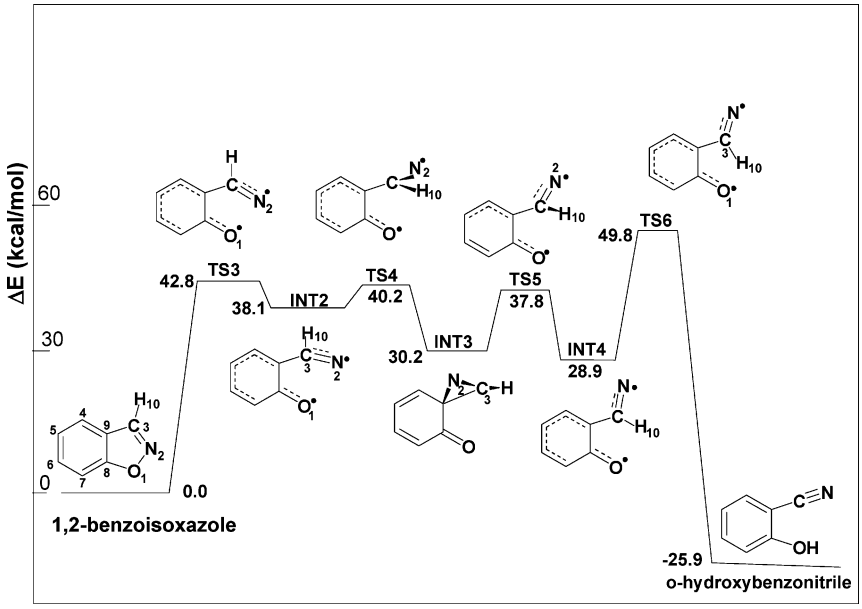

Figure 8. Reaction pathway for 1,2-benzisoxazole → *o*-hydroxybenzonitrile isomerization. Relative energies (in kcal/mol) are calculated at the uCCSD(T)//uB3LYP/cc-pVDZ level of theory. The surface has three intermediates and four transition states. The isomerization rate constant calculated on the basis of surface II is in reasonable agreement with the experimental rate constant.

TABLE 3: Several Structural Parameters of the Species Involved in the Reaction 1,2-Benzisoxazole → *o*-Hydroxybenzonitrile (surface II) Calculated at the B3LYP/cc-pVDZ Level of Theory

parameter[a]	1,2-benzisoxazole	TS3	INT2	TS4	INT3	TS5	INT4	TS6	*o*-hydroxybenzonitrile
O(1)−N(2)	1.406	2.374	2.772	3.271					
N(2)−C(3)	1.307	1.262	1.259	1.255	1.244	1.245	1.258	1.222	1.166
C(3)−C(9)	1.437	1.465	1.477	1.501	1.480	1.487	1.480	1.477	1.432
C(9)−C(4)	1.406	1.391	1.387	1.384	1.465	1.416	1.388	1.393	1.409
C(4)−C(5)	1.391	1.401	1.409	1.410	1.354	1.379	1.405	1.397	1.390
C(5)−C(6)	1.414	1.412	1.412	1.411	1.453	1.435	1.415	1.413	1.403
C(6)−C(7)	1.393	1.384	1.379	1.379	1.356	1.366	1.378	1.384	1.392
C(7)−C(8)	1.398	1.440	1.457	1.455	1.468	1.461	1.454	1.432	1.401
C(8)−C(9)	1.403	1.440	1.470	1.466	1.509	1.484	1.454	1.444	1.416
C(8)−O(1)	1.354	1.264	1.248	1.252	1.227	1.239	1.254	1.278	1.352
N(2)−C(9)			2.459	2.417	1.604	2.034	2.435		
C(3)−H(10)							1.108	1.197	
O(1)−H(10)							2.386	1.667	0.973

[a] Distances are in Angstroms. Atom numbering is shown in Figure 8.

1,2-benzisoxazole to *o*-hydroxybenzonitrile is 49.8 kcal/mol at the uCCSD//uB3LYP/cc-pVDZ level of theory as reflected by the energy level of TS6 relative to the reactant.

VI. Calculation of the Isomerization Rate Constants

1. Rate Constant Based on Potential Energy Surface I. As the rate-determining step is the first step on the surface with a high barrier of ∼62 kcal/mol, we calculated the isomerization rate constant using the step 1,2-benzisoxazole → INT1 via transition-state TS1. Transition-state theory has been used as previously described, covering the temperature range at which the single-pulse shock-tube experiments were carried out. The rate constants were then plotted as ln k vs $1/T$ to obtain an Arrhenius type rate constant. The value obtained is $k_{\text{first}} = 3.14 \times 10^{15} \exp(-65.5 \times 10^3/RT)\ \text{s}^{-1}$. Comparison between the calculations and the experimental shock-tube results is shown in Figure 6. The filled circles are the experimental rate constants. The lower line is the Arrhenius plot with the 65.5 kcal/mol activation energy. As can be seen, it is considerably lower than the experimental points.

2. Rate Constant Based on Potential Energy Surface II. In view of the flatness of the potential energy surface from INT2 and on, we calculated the isomerization rate constant from the surface as if INT2 goes directly to *o*-hydroxybenzonitrile via transition-state TS6 with a barrier of 11.7 kcal/mol. The concentration of INT2 is taken as the equilibrium concentration of the reaction 1,2-benzisoxazole → INT2. In view of the very low barrier of the back reaction INT2 → 1,2-benzisoxazole, equilibrium is attained instantaneously relative to the experimental dwell time of 2 ms. The 11.7 kcal/mol barrier together with the 38.1 kcal/mol endothermicity of the 1,2-benzisoxazole → INT2 step is equivalent to a barrier of 49.8 kcal/mol. As described in the previous paragraph, the calculated rate constants were plotted as ln k vs $1/T$ to obtain an Arrhenius type rate constant. The value obtained is $k_{\text{first}} = 4.15 \times 10^{14} \exp(-51.7 \times 10^3/RT)\ \text{s}^{-1}$.

The upper line in Figure 6 is the calculated rate constant based on surface II. As can be seen, the value is about a factor of 2−3 higher, corresponding to ∼2 kcal/mol, and can be considered as a good agreement.

VII. Conclusions

The only product in the thermal reaction of 1,2-benzisoxazole over the temperature range 900−1040 is *o*-hydroxybenzonitrile. At higher temperatures a plethora of decomposition products are obtained with the same abundance regardless of whether

the starting material is 1,2-benzisoxazole or the isomerization product *o*-hydroxybenzonitrile.

The lack of fragmentation is in complete contrast to the thermal behavior of isoxazole, where no isomerization was observed.[23]

Two potential energy surfaces describing the isomerization of 1,2-benzisoxazole are presented. In the two surfaces breaking of the N−O bond is the first step. In one surface (surface I) the N−O bond is cleaved simultaneously with 1,2-H-atom migration, which results in a high barrier and thus does not contribute to the isomerization. In the second surface, which appears to be more complex, the first step involves cleavage of the N−O bond without H-atom migration. This results in an overall barrier that is considerably lower than the one obtained from surface I.

The agreement between the calculated rate constant and the experimental results is good.

Acknowledgment. This research was supported by grant no. 34/01-12.5 from the Israel Science Foundation (ISF), Jerusalem, Israel.

References and Notes

(1) Lifshitz, A.; Tamburu, C.; Suslensky, A.; Dubnikova, F. *J. Phys. Chem. A* **2006**, *110*, 8248.
(2) Lifshitz, A.; Tamburu, C.; Suslensky, A.; Dubnikova, F. *J. Phys. Chem. A* **2006**, *110*, 4617.
(3) Domene, C.; Jenneskens, L. W.; Fowler, P. W *Tetrahedron Lett.* **2005**, *46*, 4077.
(4) Matos, M. A.; Miranda M. S.; Morais, V. M. F.; Liebman, J. F. *Eur. J. Org. Chem.* **2004**, 3340.
(5) Lifshitz, A.; Shweky, I.; Kiefer, J. H.; Sidhu, S. S. In *Shock Waves*; Proceedings of the 18th International Symposium on Shock Waves, Sendia, Japan, 1991; Takayama, K. Ed.; Springer-Verlag: Berlin, 1992; p 825.
(6) Tsang, W.; Lifshitz, A. *Int. J. Chem. Kinet.* **1998**, *30*, 621.
(7) Maquestiau, A.; Van Haverbeke, Y.; Flammang, R.; Pierard, J. *Belg. Bull. Chim. Belg.* **1975**, *84*, 207.
(8) Becke, A. D. *J. Chem. Phys.* **1993**, *98*, 5648.
(9) Lee, C.; Yang, W.; Parr, R. G. *Phys. Rev.* **1988**, *B37*, 785.
(10) Dunning, T. H., Jr. *J. Chem. Phys.* **1989**, *90*, 107.
(11) Peng, C.; Schlegel, H. B. *Isr. J. Chem.* **1993**, *33*, 449.
(12) Pople, J. A.; Head-Gordon, M.; Raghavachari, K. J. *J. Chem. Phys.* **1987**, *87*, 5968.
(13) Lee, T. J.; Taylor, P. R. *Int. J. Quantum Chem. Symp.* **1989**, *23*, 199.
(14) Lee, T. J.; Rendell, A. P.; Taylor, P. R. *J. Phys. Chem.* **1990**, *94*, 5463.
(15) Bartlett, R. J. *J. Phys. Chem.* **1989**, *93*, 1697.
(16) Cramer, C. J.; Nash, J. J.; Squires, R. R. *Chem. Phys. Lett.* **1997**, *277*, 311.
(17) Kraka, E.; Cremer, D. *J. Am. Chem. Soc.* **1994**, *116*, 4929.
(18) Frisch, M. J.; Trucks, G. W.; Schlegel, H. B.; Scuseria, G. E.; Robb, M. A.; Cheeseman, J. R.; Zakrzewski, V. G.; Montgomery, J. A., Jr.; Stratmann, R. E.; Burant, J. C.; Dapprich, S.; Millam, J. M.; Daniels, A. D.; Kudin, K. N.; Strain, M. C.; Farkas, O.; Tomasi, J.; Barone, V.; Cossi, M.; Cammi, R.; Mennucci, B.; Pomelli, C.; Adamo, C.; Clifford, S.; Ochterski, J.; Petersson, G. A.; Ayala, P. Y.; Cui, Q.; Morokuma, K.; Malick, D. K.; Rabuck, A. D.; Raghavachari, K.; Foresman, J. B.; Cioslowski, J.; Ortiz, J. V.; Stefanov, B. B.; Liu, G.; Liashenko, A.; Piskorz, P.; Komaromi, I.; Gomperts, R.; Martin, R. L.; Fox, D. J.; Keith, T.; Al-Laham, M. A.; Peng, C. Y.; Nanayakkara, A.; Gonzalez, C.; Challacombe, M.; Gill, P. M. W.; Johnson, B. G.; Chen, W.; Wong, M. W.; Andres, J. L.; Head-Gordon, M.; Replogle, E. S.; Pople, J. A. *Gaussian 98*, revision A.7; Gaussian, Inc.: Pittsburgh, PA, 1998.
(19) Eyring, H. *J. Chem. Phys.* **1935**, *3*, 107.
(20) Evans, M. G.; Polanyi, M. *Trans. Faraday Soc.* **1935**, *31*, 875.
(21) Higgins, J.; Zhou, X.; Liu, R. *J. Phys. Chem. A* **1997**, *101*, 7231.
(22) Dubnikova, F.; Lifshitz, A. *J. Phys. Chem. A* **2002**, *106*, 9278.
(23) Lifshitz, A.; Wohlfeiler, D. *J. Phys. Chem. A* **1992**, *96*, 4505.